To
Bill Heetderks
Oct 7, 1997
11/26/97

Prepared for the National Institutes of Health
National Institute of Neurological Disorders and Stroke
Division of Fundamental Neurosciences
Neural Prosthesis Program
Bethesda, MD 20892

# Unassisted Standing with Functional Neuromuscular Stimulation

## NIH-NINDS-N01-NS-6-2351

**Progress Report #3**

Period Covered:
May 1, 1997 - September 30, 1997


Principal Investigator: Ronald J. Triolo, Ph.D.[1]
Co-Principal Investigators: Robert F. Kirsch, Ph.D.[2]
John A. Davis, Jr., M.D.[1]

Departments of Orthopaedics[1] and Biomedical Engineering[2]
Case Western Reserve University
Cleveland, OH 44106-4912

Co-Investigators: James J. Abbas, Ph.D.
University of Kentucky

Scott L. Delp, Ph.D.
Northwestern University


THIS QPR IS BEING SENT TO YOU BEFORE IT HAS BEEN REVIEWED BY THE STAFF OF THE NEURAL PROSTHESIS PROGRAM.

## I. ABSTRACT

The long-term goal of this contract is to develop methods to provide brace-free, energy efficient standing for persons with complete thoracic level spinal cord injuries via functional neuromuscular stimulation (FNS). The resulting system will resist reasonable disturbances and maintain balance automatically while allowing free use of the upper extremities to manipulate objects in the environment. These objectives are being addressed through an organized effort consisting of anatomical and dynamic modeling, control simulation and optimization, and experimental demonstration of new control structures. The work represents an active partnership between investigators at Case Western Reserve University (CWRU) and collaborators at Northwestern University and the University of Kentucky.

## II. INTRODUCTION

Achieving independent, hands-free standing with FNS depends upon the development of an anatomical and dynamic model of the lower extremities and torso. This model will be employed to construct dynamic simulations and perform optimization procedures to investigate the theoretical behavior of various FNS control systems for providing automatic postural adjustments. Goals for the first year of the contract include creating a new anatomical model of the trunk and integrating it into an existing three-dimensional representation of the lower extremities, adding inertial properties and developing the facility to compute dynamics, simulate the actions of FNS and optimize controller performance. Predictions resulting from the modeling and simulation will drive the implementation and experimental demonstration of the postural control systems in human volunteers.

Substantive progress has been made in modeling the musculoskeletal anatomy of the trunk, simulating feedback control using the dynamic bipedial lower extremity model, predicting the disturbances caused by voluntary upper extremity movements, and demonstrating adaptation mechanisms to account for individual variations or non-linear or time-varying processes. In addition, methods for validating the dynamic model and characterizing input devices for user-driven command of posture have been established in preparation for human trials of the first of control systems for unassisted standing. This report summarizes these results and their relationship to the overall goals of the contract.

## III. PROGRESS THIS REPORTING PERIOD

Progress this reporting period was made primarily in three areas: 1) anatomical modeling of the torso, 2) dynamic modeling and simulation, and 3) development of adaptive and command-driven preparatory components.

### A. Anatomical Modeling of the Torso

Earlier this year a preliminary model of the trunk was developed and integrated with the existing bipedal representation of the lower extremities using Software for Interactive Musculoskeletal Modeling (SIMM - Musculographics, Inc.). Vertebrae and ribs from a physical model of the trunk were digitized and scaled to represent average proportions. The resulting

skeletal model was compared to published norms and found to be accurate in terms of shoulder, pelvis and overall height. The geometries of the individual vertebrae were also compared to previously published data. Dimensions of the thoracic vertebrae (anterior and posterior vetebral body height and transverse process width) were within one standard deviation of population norms, while the dimensions of the lumbar segments were slightly larger than published averages. Overall, the skeletal components of the model were found to be in good agreement with data appearing in the anatomical and biomechanical literature. The origins and insertions of the erector spinae (iliocostalis lumborum, logissimus thoracis and spinalis components), quadratus lumborum and rectus abdominus were determined from anatomical drawings, CT/MRI images and cadaver dissection. These muscles were also incorporated into the SIMM model. Details of the preliminary torso model were presented in Progress Report #2 (January 1, 1997 – April 30, 1997).

The past three months were dedicated to 1) refining the estimates of muscle moment arms, 2) modeling motion at the vertebral joints, and 3) initiating data collection on muscle architecture and other parameters required to compute the moment generating capacity of the muscles through quantitative cadaver dissections.

*1. **Estimating muscle moment arms:*** Since last report, the moment arms of the three trunk muscle groups (erector spinae, quadratus lumborum and rectus abdominus) in the upright standing position were re-computed and compared to published values. The erector spinae was represented as three separate segments (on each side), each with individual attachments and lines of action. The rectus abdominus was also represented as three distinct segments, while the quadratus lumborum was represented using five segments. **Figure 1** shows the moment arms of the individual muscle segments predicted with the model at the level of L2/L3. Mean moment arm values measured in cadaver studies reported by Moga et al. [1] and Tracy et al. [2] are also depicted on the figure. The moment arms computed from the model show good agreement with the average values published in the literature.

**Figure 1:** Comparison of computed moment arms predicted by the model to published values measured at L2-L3. Left-right symmetry is assumed and only unilateral data are depicted. Analysis shows good agreement between the model and measured values reported in the literature.

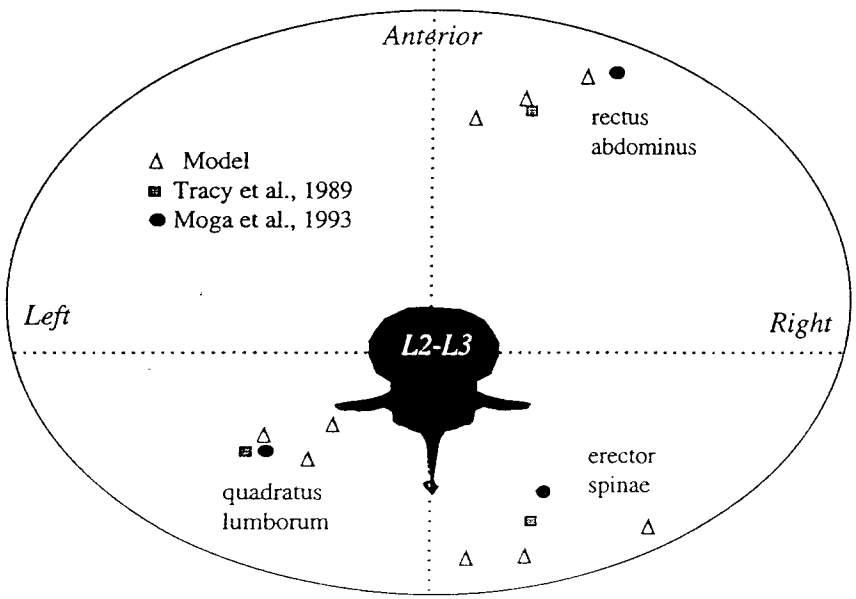

2. ***Modeling spinal motion:*** Relative motion of the spine was modeled after data reported in the literature by Panjabi and White [3]. The distribution of spinal motion is illustrated in **Figure 2.** Flexion-extension occurs primarily at the lumbar region, while axial rotation occurs primarily over thoracic levels. Axial rotation is distributed relatively evenly across all vertebrae. The model distributes motions along the spine in proportion to the relative contributions described by this relationship. For example, a given axial rotation of the trunk is achieved with relatively more motion in the thorax than lower back in accordance with values depicted in the figure. This tightly couples the motions of the individual vertebrae, which rarely move individually in life.

**Figure 2:** Distribution of movements over spinal levels. Motions in the model are distributed in this manner, rather than by representing each vertebral joint independently.

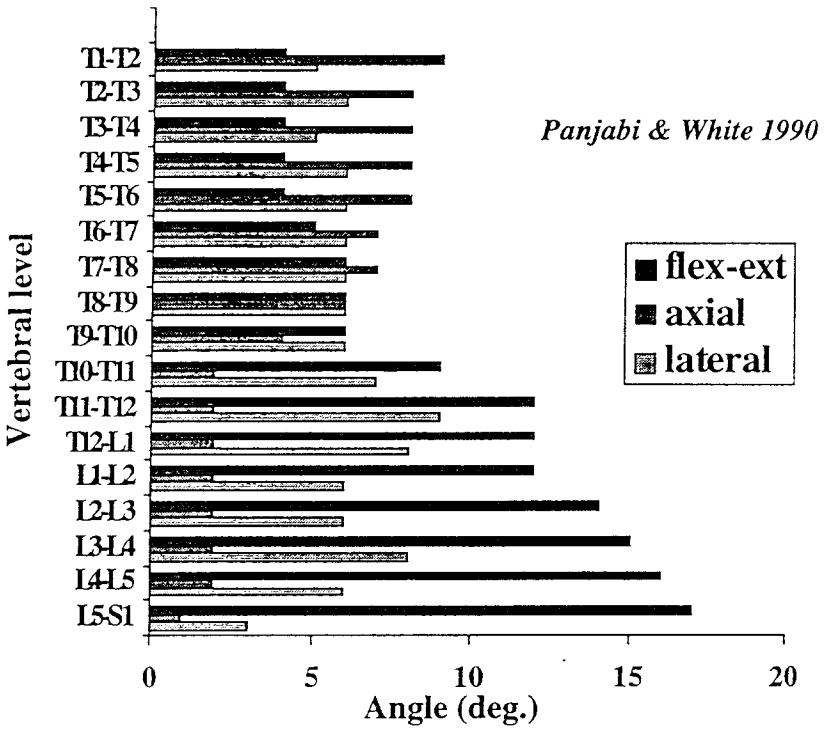


3. ***Determining muscle architecture and model parameters:*** No citations in the literature were found that describe the parameters required to model the geometry and contractile properties of the trunk muscles and characterize their force producing capabilities. As per the work plan and research schedule outlined for the first contract year, we initiated a series of original anatomical studies on fresh frozen cadavers to determine these parameters.

Experiments were performed at MetroHealth Medical Center and at Northwestern University to measure architectural parameters from quadratus lumborum, rectus abdominus, and each of the three columns of the erector spinae (spinalis thoracis, longissimus thoracis, and illiocostalis lumborum). The first cadaver dissection was completed in Cleveland by investigators from CWRU and Northwestern. First, the skin, subcutaneous fat and superficial muscles of the shoulder (latissimus dorsi, trapesius) were removed to expose the erector spinae. Each column of the muscle group was carefully removed from its bony attachments. **Figure 3a** shows the spinalis isolated from the fibers of the iliocostalis lumborum during the dissection. Detailed anatomical descriptions, drawings, and photographs were collected as each muscle was revealed. The origin and insertion, various attachments, and physical dimensions of each muscle was recorded. The muscles along with their aponeuroses, tendons, and tendinous slips were harvested. Drawings and photographs were also made (after harvesting) before fixing the

muscles in 10% formaldehyde. This procedure was repeated for the quadratus lumborum and rectus abdominus. The muscle samples were transported to Chicago for further analysis.

A protocol for measuring morphometric parameters, such as physiologic cross sectional area (PCSA), fascicle length, musculo-tendon length, sarcomere length, and pennation angle was established at Northwestern University. To date we have completed the measurements on three muscle segments (spinalis thoracis, and two segments quadratus lumborum) according to this procedure. The muscles were rinsed in phosphate buffer for a period of 24-48 hrs. They were then placed in 15% sulfuric acid for 24-72 hrs to remove fascia, followed by soaking in the phosphate buffer for at least 24 hrs a second time to neutralize the acid. The physical dimensions of the muscles were then measured. Drawings of the origin, insertion, orientation, and pennation of the fibers were recorded, along with the muscle line of action. Musclo-tendon lengths were measured as the distances between the most proximal and distal tendons for each muscle, and muscle lengths were recorded as the distance between the most proximal and distal muscle fibers. Pennation angles were measured as the angle made by the fibers with the tendons using a goniometer. The muscles were then divided into segments as represented in the musculoskeletal model. Ten fascicles were removed from each segment, making a note of the location and length of each fascicle. **Figure 3b** illustrates this step in the post-dissection analysis of the spinalis specimen. The angle of pennation is clearly visible and a single muscle fascicle has been removed for measurement.

**Figure 3:** Dissection and analysis of trunk muscles to determine architectural parameters for the model. (a) Spinalis thoracis muscle localized in fresh-frozen cadaver specimen. Lateral border with longissimus thoracis and T8 (right most) and T12 vertebrae are shown. (b) Spinalis isolated for analysis. Pennation angle, fascicle length and fascicular attachments are indicated.

(a) (b)

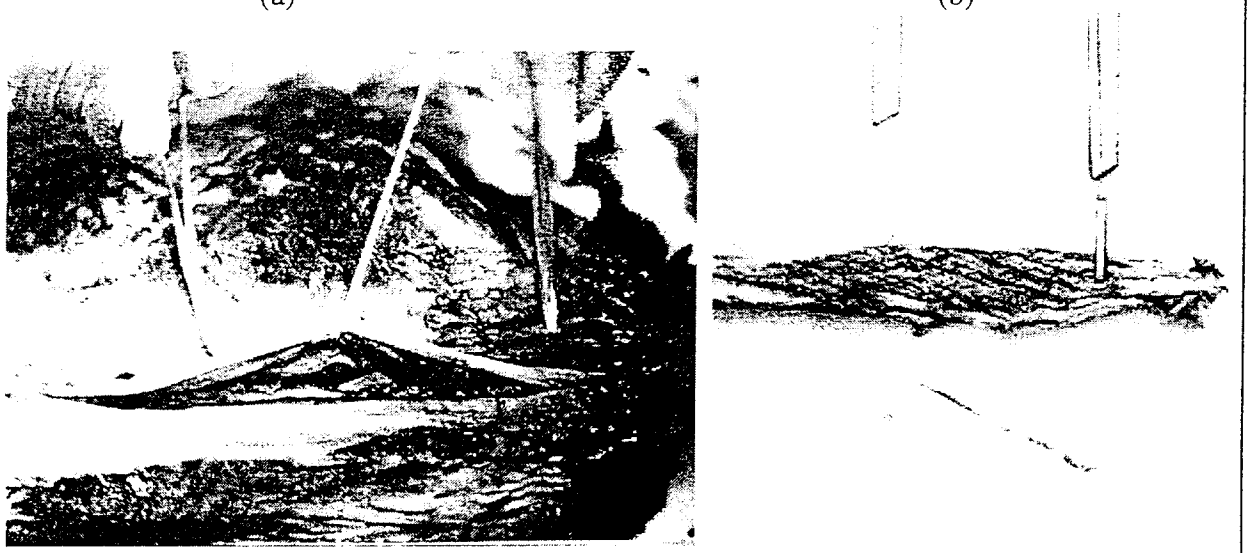

Laser diffraction was used to determine sarcomere lengths. Each fascicle was divided into a proximal, a middle, and a distal portion. A very small piece of fascicle from each portion was set on a microscope slide and a 5 mW laser was passed through it to form a diffraction pattern. Three patterns were studied for the origin portion, six for middle, and three for the

insertion portion (12 for each fascicle). The width of the first order pattern was measured and used to calculate the sarcomere length. The mass of the muscle and the optimal fascicle length were then measured to calculate PCSA.

Model parameters from the first set of muscle specimens are summarized in **Table I**. All measurements are in centimeters unless otherwise indicated. Initial analysis suggests that optimal fascicle length of the spinalis is equal to its resting length, indicating that maximal force will be produced when the trunk is in the erect position.

**Table I:** Completed Analysis of Morphometric Parameters for Trunk Muscles

| **Muscle Segment** | **Measured Muscle Parameters** | | | | | | |
|---|---|---|---|---|---|---|---|
| | Musculo -tendon Length | Muscle Length | Pennation Angle (degrees) | Fascicle Length (n=10) | Sarcomere Length μm (n=120) | Optimal Fascicle Length | PCSA ($cm^2$) |
| Spinalis Thoracis | 25 | 14 | 0-20 | 5.22 ± 1.06 | 2.51 ± 0.05 | 5.22 ± 1.04 | 0.88 |
| Proximal Quadratus Lumborum | 13.7 | 10.5 | 0-5 | 6.24 ± 0.44 | 2.99 ± 0.11 | 5.13 ± 0.42 | 1.09 |
| Distal Quadratus Lumborum | 8.5 | 8.4 | 0-5 | 4.24 ± 0.90 | 2.89 ± 0.14 | 3.64 ± 0.68 | 0.92 |

Measurement of the morphometric parameter of the other specimens is currently underway. Additional dissections and analyses will continue through the next contract year. We anticipate collecting specimens from other cadavers and incorporating the muscle parameters into the torso model in SIMM. These original contributions should also be suitable for publication.

### B. Biomechanical Modeling and Simulation

In the previous period, we reported the implementation of a dynamic, three-dimensional, 12 degrees-of-freedom, closed-chain model of the two human lower extremities. Techniques that were developed to allow stable simulations to be performed with this model in the presence of kinematic measurement noise and numerical errors (such as round-off) were also described. Activities during the current period focused on demonstrating the feasibility of performing closed-loop feedback control simulations with the computer model and on developing the infrastructure and methods for validating the model experimentally.

***1. Simulation of a joint angle-based feedback controller for maintaining upright balance.*** Using the bipedal lower extremity model, a feedback controller based on measurement and maintenance of joint angles (illustrated schematically in **Figure 4**) was implemented in simulation. The full three-dimensional model was used in this preliminary simulation, but for simplicity all disturbances were restricted to the sagittal plane. Because the properties of the musculature were assumed to be symmetric for the two lower extremities, the motions resulting from the sagittal plane disturbances were thus also confined to the sagittal plane. Note that both the sagittal plane restriction on disturbances and the assumption of symmetry of the musculature were imposed only for this initial simulation and are *not* features of the model.

As shown in **Figure 4**, a feedback control system based on joint angles was superimposed upon the musculoskeletal model. Because disturbances were limited to the sagittal plane, only 6 joint angles (bilateral hip flexion-extension, knee flexion-extension, and ankle flexion-extension) were used as feedback variables. Furthermore, we assumed that all of the joint angles could be measured perfectly, i.e., no models of realistic sensors have yet been incorporated. Each of the joint angle variables were subtracted from the desired joint angles (which were chosen to produce a desired upright posture), and the resulting difference signals were then input into 6 separate proportional-integral-derivative (PID) controllers. Thus, although we assumed perfect knowledge of joint angle, we did not assume that joint angular velocities or accelerations were measured. The error signal output by each of the PID controllers was then used to modify the activations of the muscles crossing its controlled joint according to the relative strength of each muscle. Specifically, the error signals were converted into contributions to muscle activations by weighting each muscle according to the maximum joint moment that it could produce at a joint with the joint in its desired position. An overall scaling factor common to all muscles was selected by trial-and-error to limit total activation below maximum (1.0) and to produce a stable response to a disturbance (see below). The set of muscle activations computed at each 1 ms time step of the simulation was then input to the three-dimensional musculoskeletal model to compute the forces and motions generated across time by disturbances and by the changes in muscle activation patterns produced by the controller to resist the disturbances.

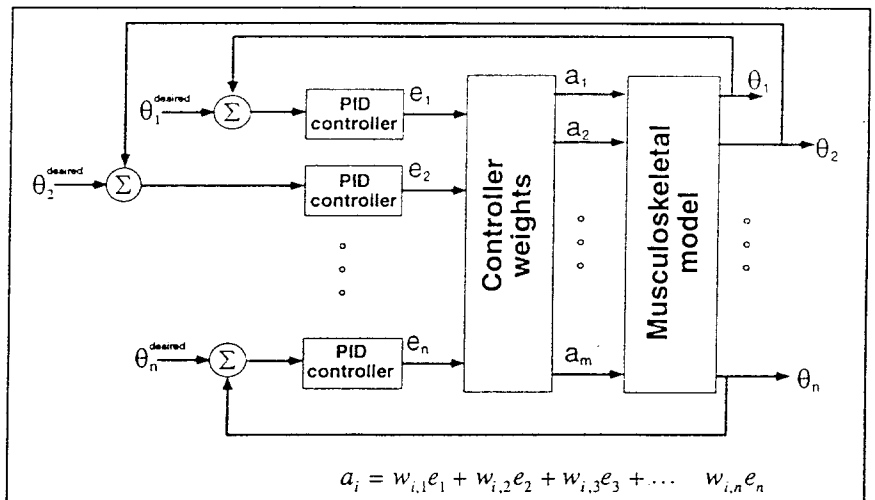


**Figure 4:** Joint angle feedback controller schematic

The result of one such simulation is illustrated in **Figure 5**. In this simulation, the disturbance used was a backward-leaning initial position (trunk extended 10 degrees past vertical, knee flexed 20 degrees, and the ankle dorsiflexed 10 degrees) that was identical for each of the two legs. For this simulation, all 23 muscles bilaterally (46 total) were used. The muscles were initially unactivated, but the final solution required each of the muscles to be activated to at least 20% of maximum (see below). **Figure 5** illustrates the time course of the activations of 5 important muscles as examples, along with the corresponding joint angles. As noted above, the motions of the two legs were essentially identical, so only one set of joint angles is shown.

At the onset of simulation, the controllers sensed the postural errors and rapidly increased the activation of the soleus and rectus femoris to straighten the hip, knee, and ankle joints. After approximately 80 ms, there was a small degree of overshoot of each of the angles, but this was resisted by a modest increase in the activities of the antagonistic muscles (tibialis anterior, semimembranosus, and gluteus maximus), and each of the joint angles thereafter smoothly reached the final desired positions. Steady-state activation levels of approximately 20% of maximum across all of the muscles were found to be necessary to achieve a reasonably rapid but

smooth movement to the desired position. The need for coactivation of muscles to stabilize posture was expected, and will be incorporated to some degree in all controllers subsequently developed.

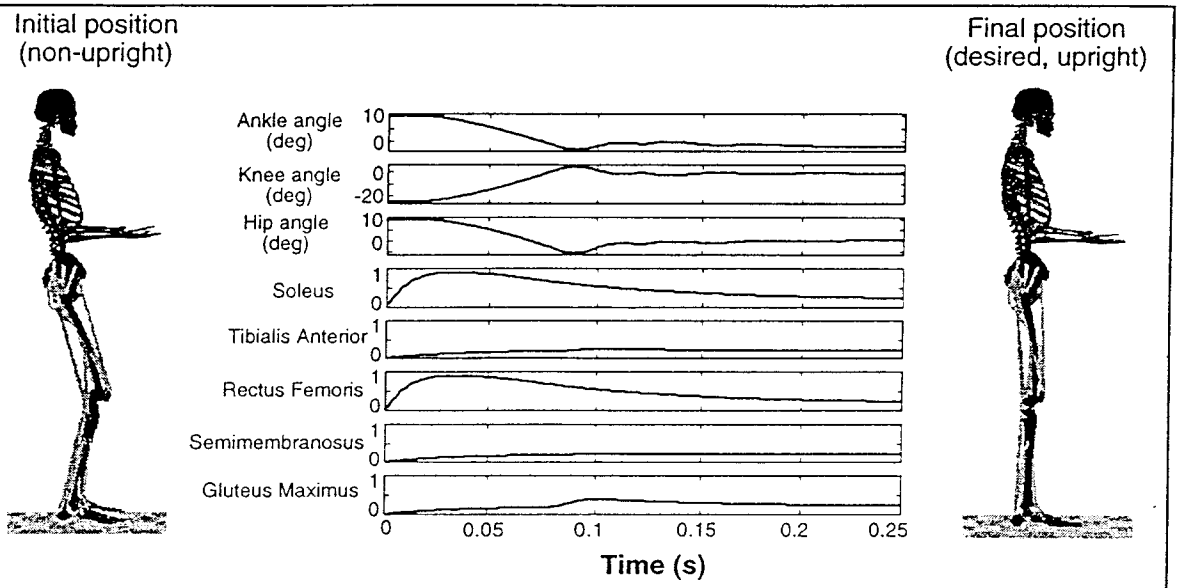


**Figure 5:** Performance of joint-angle feedback controller

The controller simulation described above demonstrated two important capabilities that are essential to the use of this model during the remainder of this project. First, the full three-dimensional, closed-chain model was successfully used to perform a numerically stable simulation. Second, a feedback controller was successfully implemented in simulation using this model, and the resulting performance was both physiologically appropriate (i.e., the timing of changes in activation and the needed coactivation levels) and encouraging. This controller simulation was limited in several aspects, however. The disturbance was limited to the sagittal plane and was of one type only (i.e., a steady-state postural error) and did not include more transient perturbations. The controller parameters (proportional, integral, and derivative gains for each of the 6 controllers, as well as the muscle activation weighting factors) were chosen by trial-and-error to produce an adequate response, but these parameters are not likely to be optimal in any sense. In the next period, we will begin to simulate more general situations (e.g., three-dimensional disturbances of various types) and will use optimization techniques to find controller parameters and coactivation levels which minimize energy consumption while producing stable posture during disturbances. We will also begin to incorporate realistic sensor properties into the model, and we will begin the evaluation of controllers using both feedforward signals as well as feedback signals other than just joint angles.

2. ***Validation of dynamic musculoskeletal model.*** During this reporting period, we devised a plan to experimentally validate the musculoskeletal model that was previously developed, and we have constructed the experimental apparatus needed to perform these experiments. The validity of the model will be tested by measuring body kinematics, the ground reaction forces at each of the feet, and the electromyographic (EMG) activity in 16 lower extremity muscles (8 bilaterally) while subjects (able-bodied initially) perform a variety of

postural adjustments during standing. An OptoTrak motion analysis system (Northern Digital, Inc.) has been set up to measure the motions of each of the segments of the lower extremities and of the trunk using a set of 20 infrared light-emitting diode (LED) "markers". Two 6-axis force platforms (AMTI, Inc.) have been obtained and mounted to a platform so as to measure the ground reaction forces and moments separately for each foot. A set of 16 EMG signals can now be measured to obtain semi-quantitative estimates of the activation level of 8 major muscles in each leg.

In the coming period, we will begin to use this setup to validate the three-dimensional closed chain model. Able-bodied subjects will be instrumented with LED markers and EMG recording electrodes, and will stand with each foot on a separate force plate. The subjects will then perform a set of leaning and squatting motions with both feet remaining in the same locations on the floor. The kinematics measured by the OptoTrak system will provide the inputs to the model, with optimization procedures used to provide the best estimate of the sequence of muscles activations needed to produce the movements. These temporal activation sequences will be then be compared to the time courses of the corresponding 16 muscle EMGs to determine if the model predictions match reality, and the reaction forces predicted by the model will be compared to those measured experimentally.

*3. Postural disturbances due to upper extremity movements:* A computer program is being developed to model the dynamics of the upper extremity in order to predict the forces and moments generated about the shoulder for functional arm movements. The purpose of this effort is to estimate the magnitudes and directions of destabilizing disturbances to posture caused by any number of volitional arm movements from simple anthropometric measurements and kinematic records. In the previous reporting period, regression equations to provide estimates of the inertial parameters of the arm were implemented (as described in McConville et al., 1980). Software to solve the equations of motion was created and performance was demonstrated with simulated data. Over the past several months, we have refined this upper extremity model, and have initiated the procedure for validating its predictions with experimental data.

The computer model of the upper extremity has now been completed and preliminary testing is underway. One major change has been implemented since the last report: the elbow joint is now modeled as a gimbal joint, rather than as a hinge. This improvement allows a more accurate representation of the position of the lower arm because it incorporates pronation/supination and the carrying angle of the forearm in the model. The program now describes both the shoulder and the elbow as three degree of freedom joints. Movements of the wrist are not included, and any load that is held in the hand is modeled as a separate segment with its own mass and inertia properties that has been attached to the hand using a zero degree of freedom weld joint.

The process for validating the model is depicted in the block diagram of **Figure 6**. First, regression equations are used to derive the inertial properties for the arm segments that are required by the model. To obtain input kinematic data, rigid bodies containing arrays of infrared LED markers are fastened to the upper and lower arm segments, and the three-dimensional coordinates of the markers are recorded using the OptoTrak system. From these coordinates, the positions of five bony landmarks (the acromion, the lateral and medial epicondyles, and the lateral and medial styloids) are derived. The bony landmark positions are used to set up local reference frames for each of the arm segments. From these local reference frames, the Euler angles that describe the orientation of one reference frame with respect to another are computed.

Three Euler angles are necessary to describe the upper arm's reference frame with respect to the ground, and three more Euler angles are needed to describe the lower arm's reference frame with respect to the upper arm. These Euler angles and their first and second derivatives (along with the inertial properties) are used as inputs to the model and are sufficient to completely describe the instantaneous position, velocity, and acceleration of the two body segments.

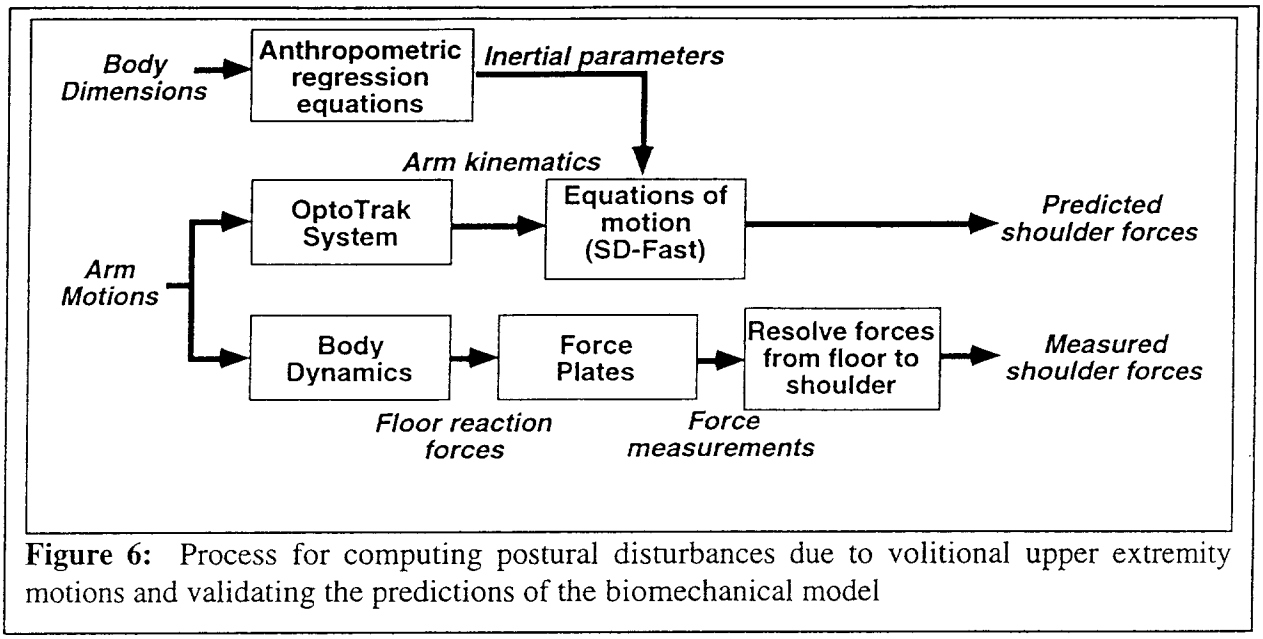


**Figure 6:** Process for computing postural disturbances due to volitional upper extremity motions and validating the predictions of the biomechanical model

To verify the model, a pilot experiment was performed in which ground reaction forces and moments were collected using the two biomechanics platforms in addition to the three-dimensional coordinate data. Providing that the rest of the body is kept in a fixed position, the ground reaction forces and moments can be combined to find the disturbances generated at the shoulder due to an arm movement. With a pilot subject seated for the trials to insure that the movement of the body was negligible, the output of the model was compared to the data from the force platforms. This experimental set up for these preliminary validation trials is pictured in **Figure 7**.

Three types of movements were performed with the subject holding a five-pound (2.268 kg) weight in his hand: sagittal plane movements, transverse plane movements and free random movements. The subject was instructed to perform each arm movement at the most rapid rate possible without causing noticeable movement of the body. These rapid, loaded conditions cause the greatest postural disturbances due to the increased mass of the arm system and increased dynamic contributions. The global axes were defined so that the X-axis points anteriorly, the Y-axis points upward, opposite the direction of gravity, and the Z-axis points laterally. This describes a right-handed coordinate system. For the pilot experiment, the mass of the upper and lower arm segments was found to be approximately 4.480 kg using the regression equations, so that the combined weight of the modeled system (the arm plus the five-pound load) was 66.18 Newtons. The Y-axis force will always contain a negative component equal to the weight of the arm system.

The output of the model compares favorably with the recorded data. For the sagittal movements, shown in **Figure 8**, the subject was instructed to hold the elbow in extension, so that the whole arm moved as a simple pendulum, swinging in a vertical plane that passed through the

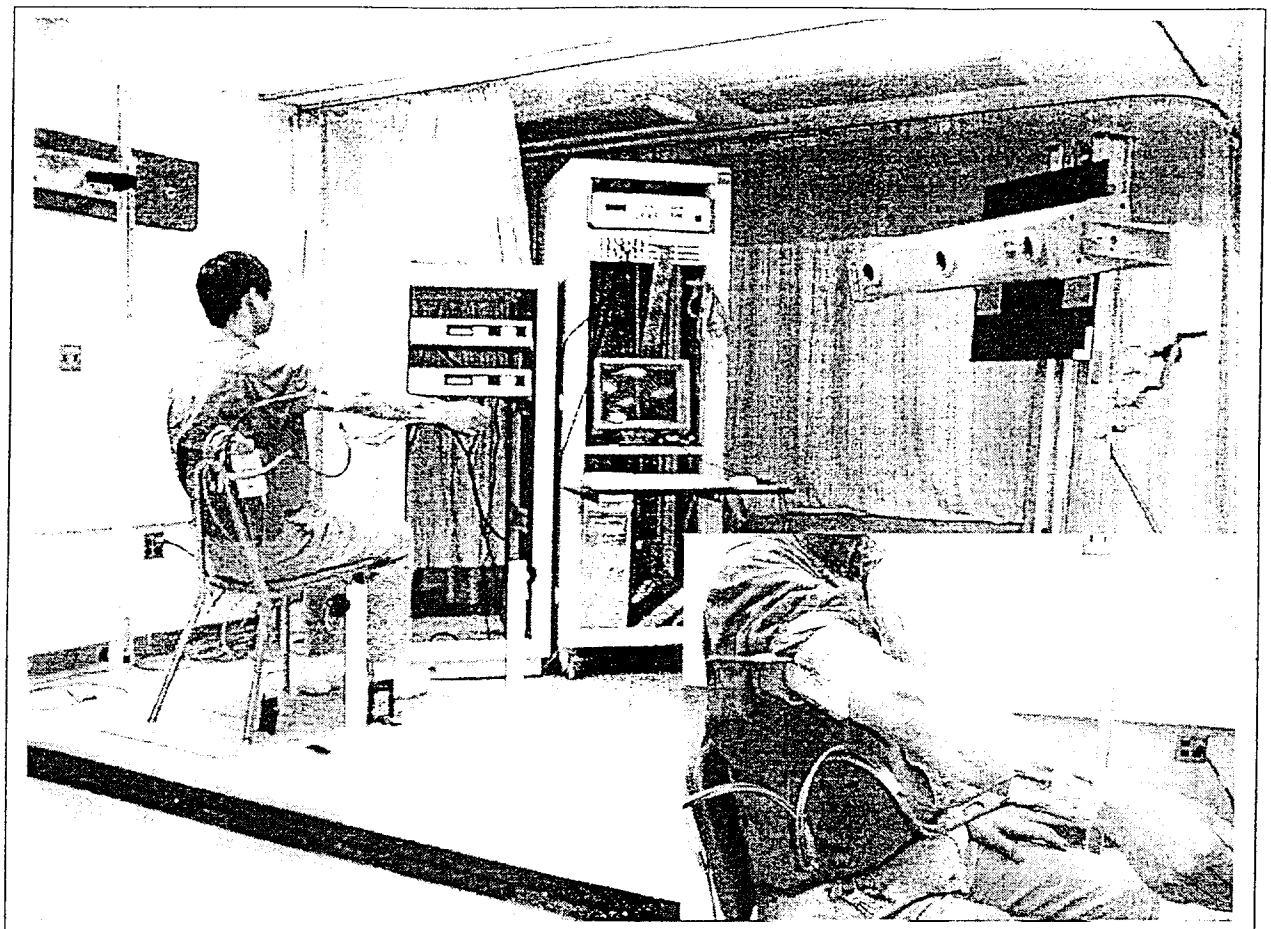

**Figure 7:** Experimental validation of the dynamic upper extremity model. Subject is seated on biomechanics platforms in order to refer the recorded ground reactions to the shoulder. Upper extremity motion is monitored by arrays of LEDs (insert) and referred to bony landmarks. Kinematic data and inertial properties are combined to predict shoulder forces and moments which are compared to the data recorded by the forceplates.

shoulder. This movement resulted in force disturbances in the X and Y directions only, with only very small perturbations in the Z direction. The moments about the Z-axis are large, which is to be expected since that is the axis about which the arm is swinging. The moments about the X and Y-axes are negligible. For the transverse movements (not pictured), the elbow was held in extension while the arm was pivoted about the Y-axis, moving in a horizontal plane that passed through the shoulder. For these movements, the greatest fluctuations in force occurred in the X and Z directions, while the fluctuations in the Y direction forces were very small. As in the sagittal movements, the large moments occurred about the axis of rotation (in this case, the Y-axis). However, for these movements, the moments about the X-axis went from positive to negative as the arm was moved from one side of the X-axis to the other. The changes in moments about the Z-axis were much smaller because the position of the arm was always nearly perpendicular to the Z-axis. For the random movements (not pictured), the position of the hand traced out an imaginary figure-8 in front of the subject. The subject was instructed to move the elbow freely as desired. The resulting forces and moments are fairly equal in magnitude for all of the axes, which is to be expected due to the nature of the movement.

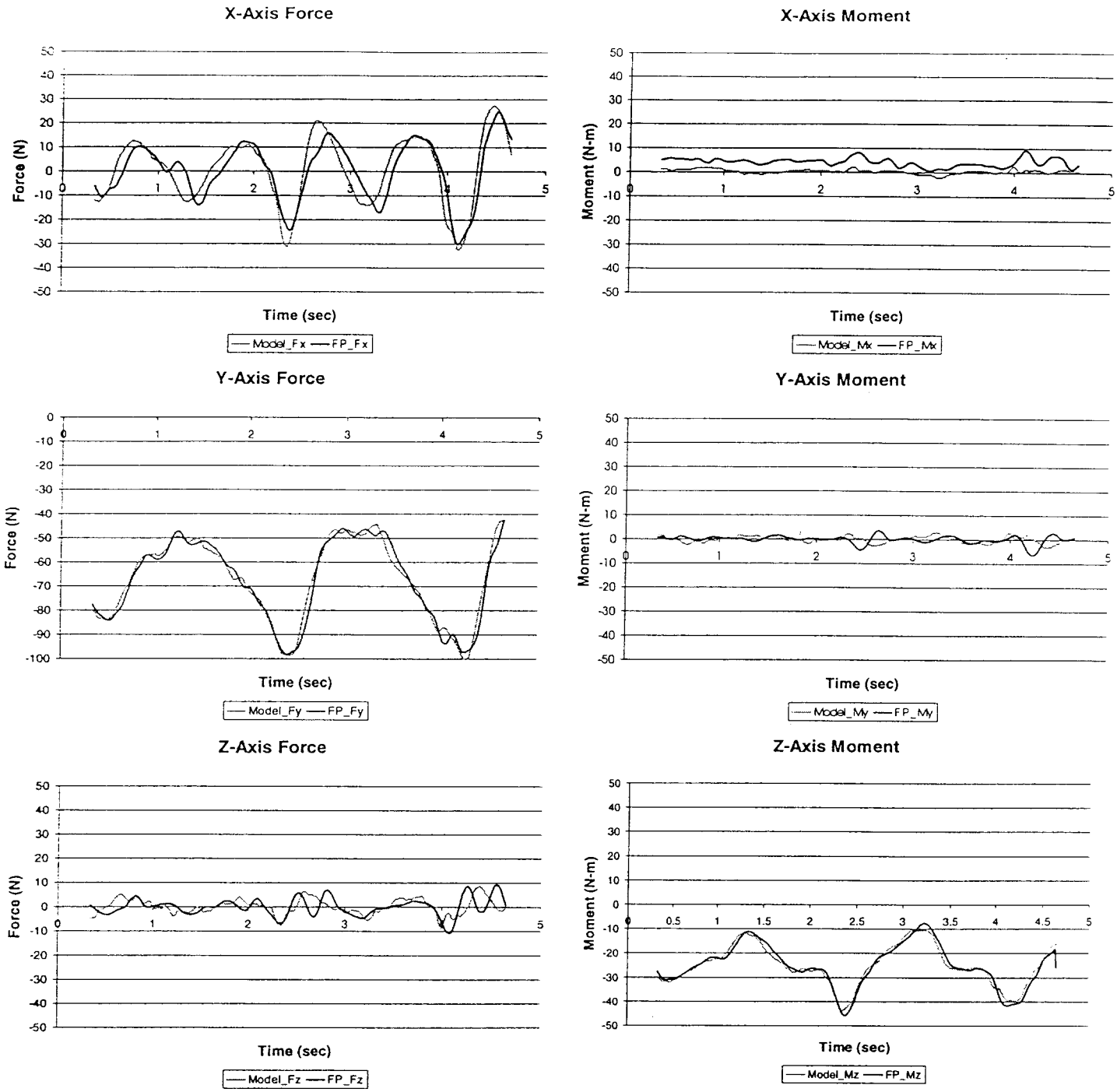


**Figure 8:** Model output for fast, loaded movements in the sagittal plane. A five-pound weight was held in the hand while the arm was swung like a pendulum about the shoulder with the elbow extended. Predicted and measured forces along the X (anterior-posterior), Y (cephalo-caudal) and Z (lateral-medial) axes are depicted in the first column and moments are given in the second column. There is good agreement between predicted (Model) and observed (FP) shoulder disturbances. As expected from the nature of the movement, Z axis force and both X and Y moments are negligible. Effects of gravity are evident in Y force and Z moment offsets

The output of the model demonstrates good correlation with the force platform data for all three types of movements and shows promise toward fulfilling the function for which it is intended – predicting the postural disturbances due to upper extremity activities. The next step in this section of the project is to collect data from other able-bodied subjects after human study approval is obtained. Some data will be recorded with the subject seated on the force platform, performing arm movements similar to the ones described above. This data will be used to further validate the model and prove that it can be used to predict the period and amplitude of postural disturbances robustly for a variety of individuals. New data will also be collected with the subjects standing and performing typical, bimanual tasks. These data will be used to specify the nature of postural disturbances that must be counteracted by the FES control system.

The sample data show how the dynamics of arm movements can affect the forces and moments that are generated at the shoulder. Variations in speed, position, and load can dramatically affect the magnitude of resulting disturbances. We plan to study what types of disturbances will occur due to unexpected changes in load and the arm movements that result from these changes, and to validate these predictions with experimental data.

### C. Adaptive and Preparatory Control Development

In previous contract work, we had established the ability of an adaptive algorithm to account for nonlinear and time-varying muscle properties in a quasi-static simulated single-muscle system. In this contract period, the adaptive control system was interfaced with a dynamic musculoskeletal model and the evaluation of the algorithm's ability to account for variations in dynamic properties was initiated. This adaptive component represents one of our approaches to individualizing control systems for each user without constructing detailed personal models for every human volunteer, as well as to account for the effects of fatigue or non-ideal operating conditions. Progress was also made on one control strategy for user command-driven selection of posture in preparation for functional reaching tasks or anticipated disturbances. The preparatory control system will utilize an input device to provide the user with a means of adjusting stimulation parameters. In this contract period, we have developed software to be used to evaluate candidate user input devices.

*1. Adaptive controller implementation for a dynamic musculoskeletal model:* Our overall control scheme includes a mapping function that transforms control signals (or input commands from the user) into stimulation parameters for various muscles. The adaptive component is designed to make automatic adjustments to this map in order to maintain linear input/output relationships and to maximize the resolution or operating range available to the control system (or to the user). The primary obstacles in achieving the linear input/output relationship are: muscle recruitment nonlinearities, muscle fatigue, and multi-joint interactions. The ability of an adaptive algorithm to account for nonlinear and time-varying muscle properties was previously established and described in the last progress report. In this contract period, we have interfaced the adaptation software with a dynamic model of a single skeletal segment acted upon by an agonist/antagonist pair of muscles to begin assessing the performance of the adaptive algorithm in simulation.

The single-segment agonist/antagonist model was implemented in the Matlab/Simulink program. The muscle model included nonlinear recruitment, length-tension and force-velocity properties. Model parameter values were selected to represent muscles at the hip acting on a swinging leg. In these initial tests, a single muscle was used to flex the leg against the action of

gravity and the desired trajectory (simulating user input of command-driven posture or output of an automatic control system) was simulated as a sequence of ramps of different velocities and terminal angles. Initially, a linear map was used to transform user input signals to stimulus pulse duration, which only scaled the nonlinearities inherent in the system proportionately. Applying the adaptive mapping scheme successfully linearized the input/output properties of the entire system (adaptive map cascaded with musculoskeletal system dynamics), as illustrated in **Figure 9a**. The figure shows the I/O characteristics of the system before and after adaptation. The output tracking performance of the system for a ramp-and-hold type input signal after the adaptation has occurred is shown in **Figure 9b**.

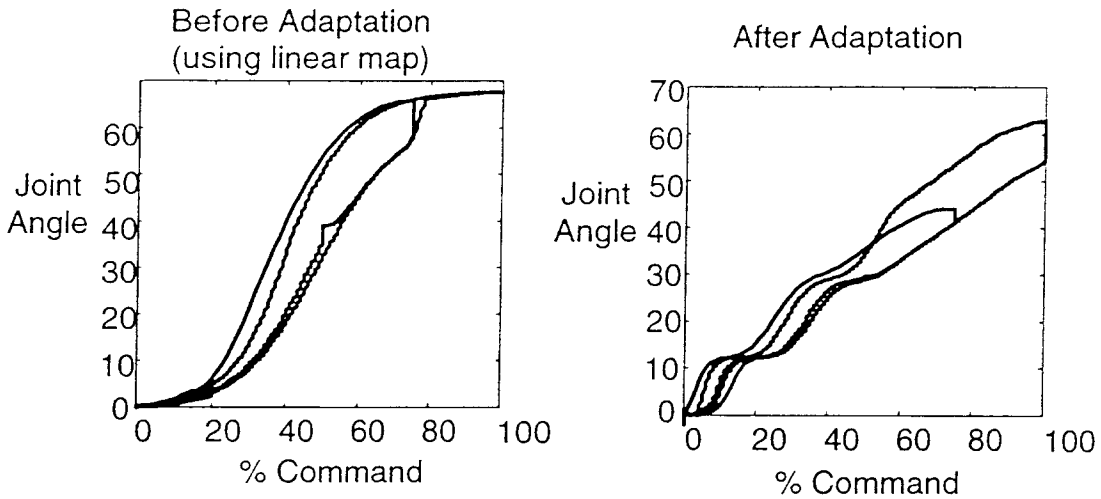


**Figure 9a:** Input/output characteristics before and after adaptation when stimulation acts on a dynamic single muscle, single joint system. The plots show that adaptation can improve the linearity of the I/O properties and utilize more of the command range.

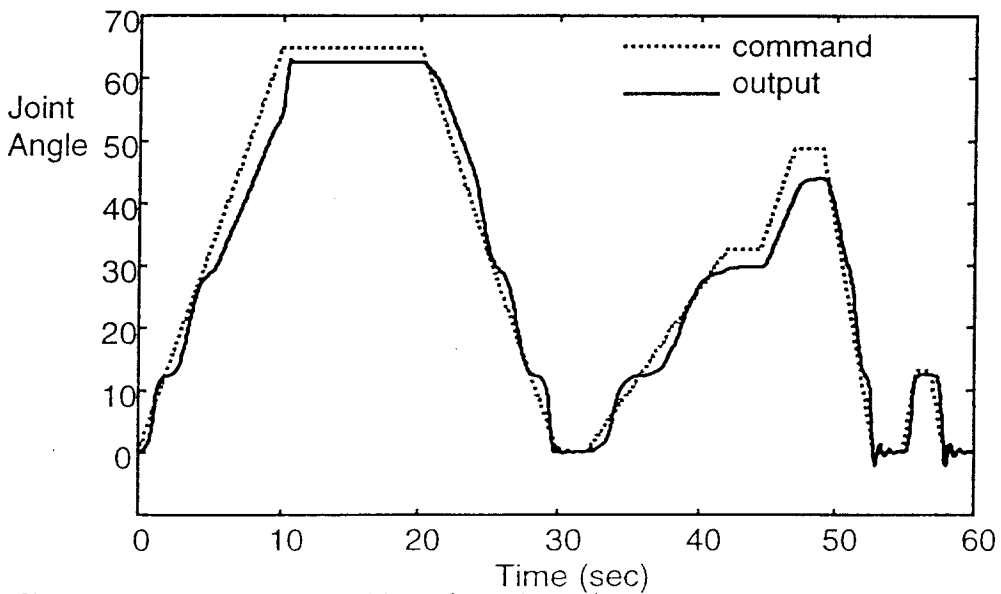


**Figure 9b:** Joint angle output tracking after adaptation.

2. *Development of a system to characterize the performance of input devices:* The "preparatory" component of our control system will provide the user with the ability to modify stimulation parameters in order to prepare for specific volitional activities or anticipated postural challenges. This requires that the user have an input device for sending information to the computer-based control system. The device should a) be capable of providing discrete as well as continuous input commands, b) be easy to use, c) provide a suitable level of input resolution, d) not interfere with functional standing activities, and e) be portable. The performance of the preparatory component of the control system will be influenced by the properties (e.g. resolution, ease of use, etc.) of the input device. In addition, we would like to have the ability to evaluate various input devices for eventual implementation in a clinical standing system.

Several studies in the literature report on the evaluation and performance of various input devices. Card, English, and Burr [5] compared the positioning time of the mouse, rate-controlled isometric joystick, step keys and text keys. MacKenzie, Sellen, and Buxton [6] compared a mouse, trackball, and a stylus in simple pointing and dragging tasks. Both studies found that the mouse performed better than its competition. These studies evaluated the ability of the user to control the position of a cursor on a screen, which responded essentially instantaneously to commands from the input device. For our purposes, however, the musculoskeletal system will introduce a significant dynamic response that may influence the choice of suitable input devices. For these reasons, we have developed software to perform experiments that are similar to those reported in the literature, with a few exceptions to better meet our objectives. In particular, we need to evaluate a wide variety of devices under different postural conditions (standing, standing with some weight supported by the arms, etc.), and we need to assess the effects of system dynamics on device performance.

A program has been developed in the Labview programming environment to perform two types of tests with various input devices: a center-out target acquisition task and a figure-8 tracking task. Any device that utilizes the computer mouse port or a game port can be used to perform the tasks. In the "normal" mode, inputs from the device are used directly to move the cursor on the screen. In the "dynamic" mode, inputs from the device are first filtered through a linear second-order system model with input delay before moving the cursor. The parameters for the second-order model were chosen to roughly approximate the response of a muscle to electrical stimulation.

In an initial set of tests with this program, we have had one (able-bodied) subject utilize three different input devices: a standard mouse, a handgrip joystick, and a portable hand-held trackball. The subject performed center-out target acquisition tasks as well as figure-8 tracking tasks. Results from target acquisition tasks (**Figure 10a**) indicate that the mouse provided the best performance ($p<0.05$) in the "normal" mode, but that it did not perform significantly better than the trackball in the "dynamic" mode. While the performance of the mouse was degraded significantly ($p<0.05$) by the inclusion of dynamics, the performance of the trackball and joystick were not significantly affected. Results from the figure-8 tracking task (**Figure 10b**) were similar: the mouse provided the best performance ($p<0.05$) in the 'normal' mode, but it did not perform significantly better than the trackball in the 'dynamic' mode. While the performance of the mouse was significantly ($p<0.05$) degraded by the inclusion of dynamics, the performance of the trackball and joystick were not affected.

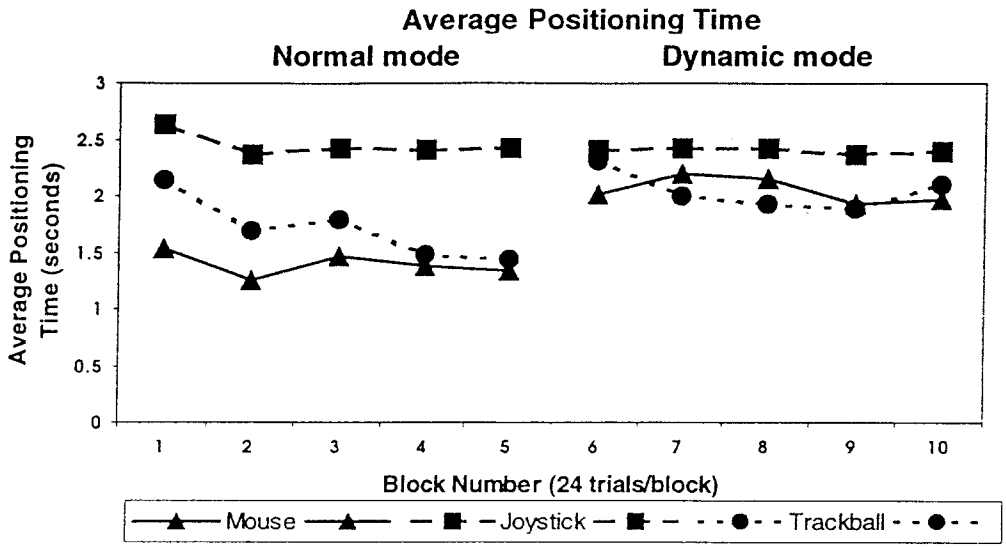


**Figure 10a:** Average positioning time for center-out target acquisition task for various input devices. The subject performed 24 trials in each of 5 blocks with each device and in each mode. 'Normal mode' indicates that the input directly specified cursor movement; 'Dynamic mode' indicates that the cursor responded as a second order system with input time delay.

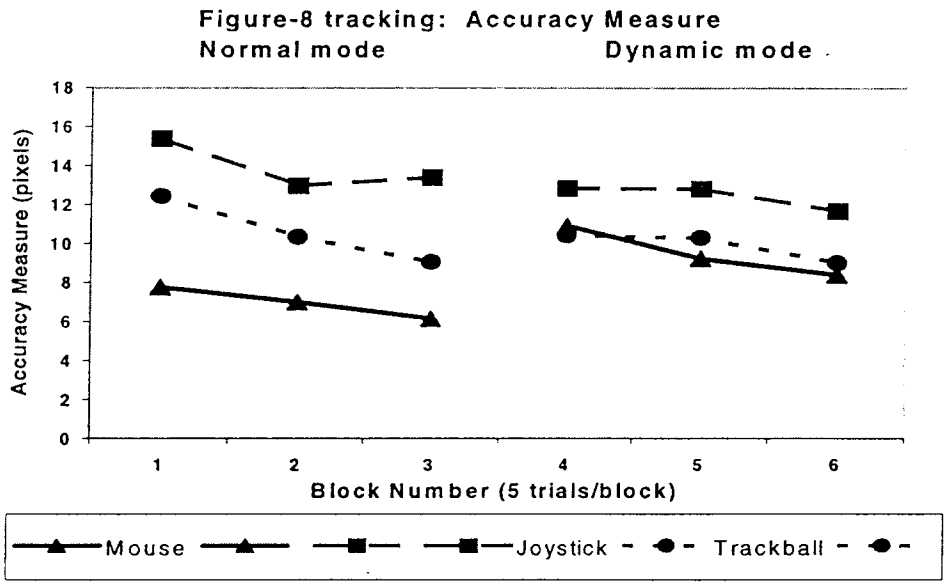


**Figure 10b:** Accuracy measures for figure-8 tracking for various input devices. The subject performed 5 trials in each of 3 blocks with each device and in each mode. 'Normal mode' indicates that the input directly specified cursor movement; 'Dynamic mode' indicates that the cursor responded as a second order system with input time delay.

Although these results are very preliminary, they suggest that the performance of some input devices may be significantly influenced by system dynamics. We are currently planning a more thorough investigation of several candidate input devices that will address issues of learning, inter-subject variability, and posture. Over the next several months, we plan to continue the evaluation of input devices, complete the setup of the laboratory hardware and software required for the experimental characterization of the open-loop control system using the posture-shifting paradigm and to begin these experiments. A secondary effort will be the continuation of the evaluation of the adaptive control system in computer simulations.

**References:**


1. Moga PJ, Erig M, Chaffin DB, Nussbaum MA: Torso muscle moment arms at intervertebral levels T10 Through L5 from CT scans on eleven male and eight female subjects, *Spine*, 18(15): 2305-2309, 1993.
2. Tracy M, Gibson MJ, Szypryt EP, Rutherford A, Corlett EN: The geometry of the muscles of the lumbar spine determined by magnetic resonance imaging, *Spine*, 14(2): 186-193, 1989.
3. White AA, Panjabi MM: Clinical Biomechanics of the Spine, 2ndedition, J.B. Lippincott Company, Philadelphia, 1990.
4. McConville JT, Churchill TD, Kaleps I, Clauser CE, Cuzzi, J (1980), Anthropometric Relationships of Body and Body Segment Moments of Inertia. AFAMRL-TR-80-119, U.S. Air Force Aerospace Medical Research Laboratory, Wright-Patterson Air Force Base, Ohio.
5. Card, SK, English WK, Burr BJ: Evaluation of mouse, rate-controlled isometric joystick, step keys, and text keys for text selection on a CRT. *Ergonomics, 21*, 601-613, 1978.
6. MacKenzie IS, Sellen A, Buxton W: A comparison of input devices in elemental pointing and dragging tasks. *Proceedings of the CHI'91 Conference on Human Factors in Computing Systems*, 161-166, 1991.